

# Optimal Portfolio of Products in a Polycrystalline Silicon Refinery

César Ramírez-Márquez, Edgar Martín-Hernández, Mariano Martín,\*  
and Juan Gabriel Segovia-Hernández\*

**Cite This:** *Ind. Eng. Chem. Res.* 2020, 59, 10552–10567

**Read Online**

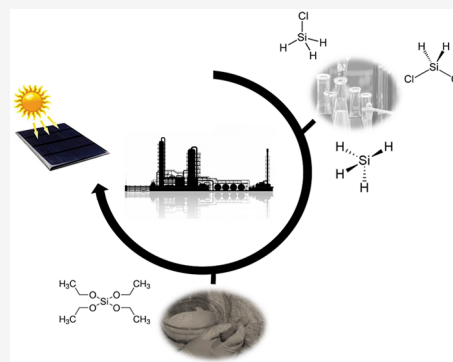
ACCESS |

Metrics & More

Article Recommendations

Supporting Information

**ABSTRACT:** The silicon industry is a source of various types of products, including materials for the implementation of renewable energy systems, with a comparatively lower environmental impact than conventional fossil energy sources and high added value byproducts. In this context, the exploitation of the different byproducts generated in the production of polycrystalline silicon (polysilicon) offers opportunities to increase the economics of the polycrystalline silicon production process. In this work, a silicon based refinery is conceptually designed using surrogate models for the major units to evaluate the portfolio of products. Although the main product is polysilicon, there are a number of products that might be obtained in the process to improve its profitability, such as tetraethoxysilane (at different purities) as well as chlorosilanes, including  $\text{SiH}_4$ ,  $\text{SiH}_2\text{Cl}_2$ , and  $\text{SiH}_3\text{Cl}$ . Next, an economic evaluation of the facility is carried out to determine its economic feasibility. The results show that the refinery produces tetraethoxysilane and chlorosilanes in addition to the production of polysilicon. The proposed design reduces the cost for polycrystalline silicon to 6.86 \$/kg, compared to a cost of 8.93 \$/kg of polycrystalline silicon if the plant does not generate high value-added byproducts, both values below the commercial price of polycrystalline silicon, which is estimated at 10 \$/kg. Therefore, the refinery is not only capable of meeting the market share requirements, but in a way that the generation of different high added value byproducts increases the plant profit compared to that of the net income earned by traditional polysilicon monoproduct plants.



## 1. INTRODUCTION

Phenomena such as climate change, resource depletion, waste generation, and pollution have prompted the industrial and academic sector to seek new and more sustainable approaches to supply energy. While there are numerous sustainable alternatives (biofuels, wind, geothermal, etc.), photovoltaic (PV) energy is considered one of the best sustainable energy alternatives.<sup>1</sup> The abundant solar radiation the Earth receives allows PV systems to meet the yearly worldwide energy needs.<sup>2</sup> Likewise, PV systems produce electricity without the need to emit pollutants during their operation, in addition to having a low carbon footprint during their life cycle, building the PV panels is superior in terms of environmental impact compared to power generation from fossil fuels.<sup>3</sup> Currently, silicon-based photovoltaic technologies are receiving more attention, as they represent the largest share in the renewable energy market, as well as it is the first renewable based power technology to be commercialized at a large scale.<sup>4</sup>

For years the PV industry was highly dependent on the availability of polycrystalline silicon as scraps from the production of integrated circuits, power devices, and discrete semiconductor devices. The photovoltaic industry used refined silicon rejections from the semiconductor device industry, which are of a slightly lower grade and, therefore, less expensive. The increased demand for PV panels has driven the development of processes for refining polycrystalline silicon.<sup>5</sup>

The refining of polycrystalline silicon is rather energy intensive and generates a large amount of residual products. However, detailed technical studies on lower cost replacement methods to produce polycrystalline silicon in recent years have failed to identify a new alternative process. There are currently two industrial processes used in the production of polycrystalline silicon. The first and former method, the Siemens process, was the only commercial route to obtain polycrystalline silicon before 1980. It remains the main technology used in the production of high quality polycrystalline silicon. The second or recent method was established in the late 1970s by Union Carbide, and it is known as the monosilane process.<sup>6</sup> To reduce the costs of polycrystalline silicon, current studies have focused on technology innovation, equipment upgrades, and process improvements. The final aim for silicon-based photovoltaic energy is to be more competitive.

Lately, the polycrystalline silicon photovoltaic (PV) industry has thrived, developing a global supply chain. In this decade alone, polycrystalline silicon-based solar panels have come to

**Received:** February 27, 2020

**Revised:** May 3, 2020

**Accepted:** May 6, 2020

**Published:** May 6, 2020





combination of the stages of the Siemens and the Union Carbide processes. In this work, the Hybrid Process is extended using a couple of reactive distillation columns for the production of high added value products such as TEOS 98.5, TEOS 99.0, TEOS 99.5, silane, dichlorosilane, and monochlorosilane. The process diagram for a multiproduct polycrystalline silicon refinery is shown in Figure 1. Table 1 shows the prices of raw materials and services required in the process.

**Table 1. Prices of Raw Materials and Utilities**

| raw material                     | price                                   |
|----------------------------------|---|
| C                                | 59.43 [\$/ton] <sup>10</sup>            |
| SiO <sub>2</sub>                 | 60.65 [\$/ton] <sup>11</sup>            |
| SiCl <sub>4</sub>                | 0.75 [\$/kg] <sup>12</sup>              |
| C <sub>2</sub> H <sub>5</sub> OH | 0.97 [\$/kg] <sup>13</sup>              |
| N <sub>2</sub>                   | 47.98 [\$/kg] <sup>14</sup>             |
| H <sub>2</sub>                   | 4.98 [\$/kg] <sup>15</sup>              |
| utilities                        |   |
| electricity                      | 0.07 [\$/kWh] <sup>16</sup>             |
| water                            | 0.33 [\$/m <sup>3</sup> ] <sup>17</sup> |
| steam                            | 0.02 [\$/kg] <sup>18</sup>              |

The process proposed consists of six stages: in the first stage, metallurgical grade silicon, Si<sub>MG</sub>, is produced (which is alike in all conventional processes) through carbothermic reduction of quartz with coal. To represent this reactor a detailed model for the reaction system considering the production of all the species of the system Si–O–C was developed. The carbothermic reduction of quartz is performed in an electric arc furnace (it can be seen in Figure 1 as Thermal carboreduction) the product distribution of which is a function of the temperature (above quartz boiling point, >2500 °C).<sup>19</sup> Once this process finishes the gases are extracted, leaving the liquid silicon at the lowermost part of the furnace. The liquid silicon is then collected, poured into the melting pot, and emptied from the bottom part of the melting pot onto the casting belt where it is solidified. The temperature at which silicon is extracted from the furnace (a critical parameter in the Si<sub>MG</sub> production) is above the silicon melting temperature.<sup>20</sup> If the temperature of silicon is too high, a premature deterioration of the refractory materials might take place, and the possibility of dissolution of gases in the liquid silicon increases. On the contrary, lower temperatures can result in low silicon fluidity (1573 K).<sup>20</sup> A suitable furnace silicon extraction temperature range is between 1590 and 1680 K. It is here, while silicon sits in the melting pot (it can be seen in Figure 1 as MP) that the refining process takes place by an oxidative process, eliminating a large part of impurities producing slag; thus, obtaining silicon with a purity of 98%–99%. Slag is eliminated either mechanically or by gravity, and stored in a container while the silicon remains in the melting pot until it reaches a temperature of around 318 and 348 K.<sup>20</sup> Various melting pots operate following a method called Sequential Casting, where successive melting pots are operated in a sequential mode and continuously feed the vessel of the steady casting system.

The molten silicon is emptied into a distribution vessel. Once the vessel is full enough to maintain a consistent feeding flow, the liquid silicon is then poured into the ingot mold. The silicon is cooled down and solidified by a series of water pipes located in the interior of the mold. Afterward, the solid silicon

is cooled once more using water showers to adjust its temperature to an adequate value of around 298 K, for the succeeding grinding in a roller crusher.<sup>21</sup> The Si<sub>MG</sub> pieces gathered after grinding are stored at atmospheric conditions in a closed silo that feeds the chlorosilane synthesis reactor.

In the second stage, recycled SiCl<sub>4</sub> is hydrogenated in a fluidized bed reactor in the presence of Si<sub>MG</sub> (it can be seen in Figure 1 as Hydrochlorination). The SiCl<sub>4</sub>–H<sub>2</sub>–Si<sub>MG</sub> system is chosen for this second stage due to the advantages related to the production of chlorosilane that include rather low operation temperatures (anywhere between 673 and 873 K) and larger silicon tetrachloride conversion.<sup>22</sup> It is in this section of the process that impurities such as Fe, Al, and B react to form their halides (e.g., FeCl<sub>3</sub>, AlCl<sub>3</sub>, and BCl<sub>3</sub>). The SiHCl<sub>3</sub> has a low boiling point of 31.8 °C, and distillation is used to purify the SiHCl<sub>3</sub> from the impurity halides. The resulting SiHCl<sub>3</sub> now has electrically active impurities (such as Al, P, B, Fe, Cu, or Au) below 1 ppba. At the conceptual design level the reactions involving them are neglected. On the basis of the experimental observations of Ding et al.,<sup>22</sup> it is assumed that in the SiCl<sub>4</sub>–H<sub>2</sub>–Si<sub>MG</sub> system the subsequent set of species is involved: SiCl<sub>4</sub>, H<sub>2</sub>, Si<sub>MG</sub>, SiHCl<sub>3</sub>, SiH<sub>2</sub>Cl<sub>2</sub>, and HCl. Hence, the operating conditions of this system are liable to be altered, disturbing the distribution of the created products. A detailed model is used to compute the effect of the operating conditions on the distribution of products.

The reactor outlet stream which contains a mixture of SiCl<sub>4</sub>, SiHCl<sub>3</sub>, SiH<sub>2</sub>Cl<sub>2</sub>, along with HCl and H<sub>2</sub>, is fed into a condensation stage that separates the reactor effluent into a gas and a liquid phase. The gas phase stream is formed by the most volatile compounds, H<sub>2</sub> and HCl, while the liquid phase stream is formed primarily by SiH<sub>2</sub>Cl<sub>2</sub>, SiHCl<sub>3</sub>, and SiCl<sub>4</sub>. Because of the large difference in volatility between hydrogen, hydrogen chloride, and the chlorosilanes, a 100% separation efficiency in this stage is considered.<sup>23</sup> Thus, the gaseous stream is cooled in the condenser until it reaches a temperature of 298 K, at which the chlorosilanes condense (it can be seen in Figure 1 as HX2). Next, the stream is introduced into a phase separator where the gaseous hydrogen and hydrogen chloride are recovered and stored in a tank. The liquid stream containing the chlorosilanes is sent to the third stage.

In the third stage, a set of convectional distillation columns is used to separate the chlorosilane mix (it can be seen in Figure 1 as CD1 and CD2). First, and due to the large quantity that it represents, the SiCl<sub>4</sub> is separated. From the top of the first distillation column, a SiH<sub>2</sub>Cl<sub>2</sub>–SiHCl<sub>3</sub> mix is recovered and fed to a second distillation column, while from the bottom high purity SiCl<sub>4</sub> is obtained. The second distillation column separates the SiH<sub>2</sub>Cl<sub>2</sub>–SiHCl<sub>3</sub> mix obtaining a high purity stream of SiH<sub>2</sub>Cl<sub>2</sub> at the top, and a high purity stream of SiHCl<sub>3</sub> at the bottom.<sup>9</sup>

In the fourth stage, the highly pure SiCl<sub>4</sub> from the first column is divided to feed a reactive distillation column that produces TEOS, and the remaining part of the stream is recycled to the hydrochlorination reactor (it can be seen in Figure 1 as RD1).

In the fifth stage, the trichlorosilane stream is divided to feed a reactive distillation column that performs the disproportion of SiHCl<sub>3</sub> into SiCl<sub>4</sub>, SiH<sub>2</sub>Cl<sub>2</sub>, and SiH<sub>3</sub>Cl. These may also be fed into the Siemens reactor (it can be seen in Figure 1 as RD2).

In the last stage, SiHCl<sub>3</sub> is fed into the Siemens vapor deposition reactor that consists of a chamber where various

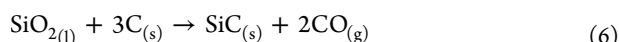
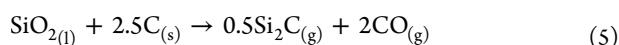
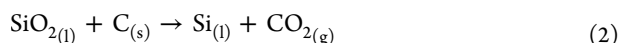
high purity silicon rods are heated by an electric current which flows through it (it can be seen in Figure 1 as Siemens). The thermal decomposition of trichlorosilane in an atmosphere of hydrogen is carried out at temperatures of 373–873 K within the reactor that leads to the deposition of silicon on the rods in the form of solar grade polysilicon.

During the deposition of the silicon, byproducts of HCl, H<sub>2</sub>, and SiCl<sub>4</sub> are obtained. A set of heat exchangers and separators is used to recover the gases. The silicon is cooled down to ambient temperature in a chamber and the gases are separated by a set of equipment, to be recycled to the process.

The process diagram for polycrystalline silicon refinery and other value-added products that are obtained in this work are shown in Figure 1, as well as the process sequence and the products generated in each stage.

**2.2. Modeling Approach.** In this section, the explanation of the development of surrogate models for the main reactors, for the distillation columns, and for the distillation reactive columns is presented. The other units: compressors, heat exchangers, mixers, and splitters are modeled based on first-principles and thermodynamics.<sup>24</sup> Most recently built silicon production plants such as Wacker and Elkem have a production capacity of 15 000 ton per year (t/y).<sup>8</sup> To achieve 15 000 t/y, in this work, a feed of 120 kmol/h of SiO<sub>2</sub> and 240 kmol/h of C is considered. The models of the thermal carboreduction, the hydrochlorination reactor, separation and purification, and deposition reactor were developed in the work of Ramírez-Márquez.<sup>25</sup>

**2.2.1. Thermal Carboreduction.** The model proposed by Wai and Hutchison<sup>19</sup> for the carboreduction of quartz has been considered to simulate the carboreduction furnace. This model takes into account the different reactions between silicon dioxide and carbon, leading to the formation of multiple products. The reactions that may take place during the silicon dioxide carboreduction process are shown in eqs 1 to 7.



On the basis of the literature<sup>8</sup> the operating conditions for the furnace consider a C/SiO<sub>2</sub> feeding molar ratio of 2:1, a total pressure of 1 atm, and a temperature range of 2500–3500 K. To model the distribution of products generated at the furnace, the phase diagram obtained by Wai and Hutchison<sup>19</sup> is used. From the figure a set of correlations were developed to estimate the mole fraction of each of the species as a function of the reaction temperature in the range from 2600 to 3100 K. These are shown in eqs 8 to 15, where  $x_i$  is the molar fraction of each species  $i$ , and  $T$  is in the temperature between the range of 2600 to 3100 K.

$$x_{\text{Si}(l)} = -2.48131 \times 10^{-9}T^3 + 1.90239 \times 10^{-5}T^2 - 4.79395 \times 10^{-2}T + 39.71359 \quad (8)$$

$$x_{\text{CO}(g)} = 9.82689 \times 10^{-5}T^3 + 1.90239 \times 10^{-5}T + 3.74066 \times 10^{-1} \quad (9)$$

$$x_{\text{Si}(g)} = 5.93093 \times 10^{-10} e^{6.31510 \times 10^{-3}T} \quad (10)$$

$$x_{\text{SiC}(s)} = 7.14539 \times 10^{-7}T^2 - 4.50044 \times 10^{-3}T + 7.08465 \quad (11)$$

$$x_{\text{Si}_2\text{C}(g)} = 1.72881 \times 10^{-7}T^2 - 9.13915 \times 10^{-4}T + 1.20759 \quad (12)$$

$$x_{\text{SiC}_2(g)} = -1.19611 \times 10^{-14}T^5 + 1.65491 \times 10^{-10}T^4 - 9.14807 \times 10^{-7}T^3 + 2.52572 \times 10^{-3}T^2 - 3.48320T + 1919.64937 \quad (13)$$

$$x_{\text{SiO}(g)} = 7.58739 \times 10^{-7}T^2 - 4.47932 \times 10^{-3}T + 6.69671 \quad (14)$$

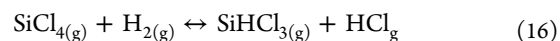
$$x_{\text{Si}_2(g)} = 4.76996 \times 10^{-13} e^{7.68303 \times 10^{-3}T} \quad (15)$$

To estimate the operation costs, the electricity consumption of electrodes (which provide the necessary energy for the reaction) is calculated formulating an energy balance using industrial data. A large consumption of power is required to melt the silica, around 10–11 kWh to produce a kilogram of silicon.<sup>26</sup>

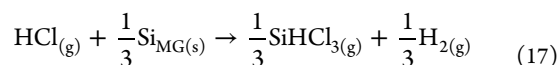
The post-processing of the liquid product obtained, mainly melted silicon, is carried out in a solidification train composed of the discharge of the melted silicon to the melting pot, the distribution pipe, the secondary cooling unit, and the roller crusher. The gaseous exit containing the gaseous effluents of the quartz carboreduction process is sent to gas treatment. The scope of the refinery model focuses on the main units that produce silicon derived products. Waste treatment, either gas or water streams, is out of the analysis. The solid SiC is extracted from the melting pot as slag, whereas the metallurgical silicon is sent to the solidification stage where it is cooled down for its subsequent use in the chlorosilane synthesis reactor.

**2.2.2. Hydrochlorination Reactor.** In this unit the hydrogenation of the recycled SiCl<sub>4</sub>, together with the Si<sub>MG</sub> is carried out, resulting in the production of chlorosilanes. The modeling of the hydrochlorination reactor is performed through the thermodynamic analysis of the SiCl<sub>4</sub>–H<sub>2</sub>–Si<sub>MG</sub> system developed by Ding et al.,<sup>22</sup> including both thermodynamic models and experimental data. The series of reactions that the proposed system considers are

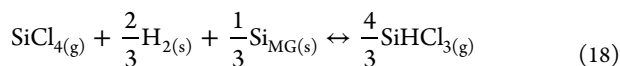
- the SiCl<sub>4</sub> hydrogenation in the gas phase, eq 16:



- and the hydrochlorination of Si<sub>MG</sub> with HCl, eq 17:



Combining eq 16 and eq 17, gives eq 18:



The model to predict the product distribution in this unit is based on the minimization of Gibbs free energy for the reactions of the  $\text{SiCl}_4\text{--H}_2\text{--Si}_{\text{MG}}$  system. It is assumed that the chemical system is ideal achieving equilibrium. The minimization of the total Gibbs free energy was modeled using GAMS and computed offline. This model is used to develop a surrogate model to be incorporated into the flowsheet optimization to predict the species molar composition as a function of the operating variables, the temperature, the pressure, and the  $\text{H}_2/\text{SiCl}_4$  molar feed ratio. A design of experiments is performed in which the range of operating variables is the following: temperature ( $T$ ), 373–873 K; pressure ( $P$ ), 1–20 atm; and  $\text{H}_2/\text{SiCl}_4$  molar feeding ratio (Rel), 1–5. The surrogate model consists of eqs 19 to 23:

$$\begin{aligned} x_{\text{SiCl}_{4(g)}} &= 5.345 \times 10^{-1} - 4.0 \times 10^{-6}P \\ &\quad - 1.6805 \times 10^{-1}\text{Rel} + 1.7367 \times 10^{-2}\text{Rel}^2 \\ &\quad + 1.0 \times 10^{-6}P \cdot \text{Rel} \end{aligned} \quad (19)$$

$$\begin{aligned} x_{\text{SiHCl}_{3(g)}} &= 2.3454 \times 10^{-1} + 4.0 \times 10^{-6}P \\ &\quad - 7.369 \times 10^{-2}\text{Rel} - 8.0 \times 10^{-6}T \\ &\quad + 7.633 \times 10^{-3}\text{Rel}^2 + 1.0 \times 10^{-6}T \cdot \text{Rel} \cdot T \end{aligned} \quad (20)$$

$$\begin{aligned} x_{\text{SiH}_2\text{Cl}_{2(g)}} &= 2.781 \times 10^{-2} + 1.0 \times 10^{-6}P \\ &\quad - 9.358 \times 10^{-3}\text{Rel} + 4.0 \times 10^{-6}T \\ &\quad + 1.031 \times 10^{-3}\text{Rel}^2 \end{aligned} \quad (21)$$

$$\begin{aligned} x_{\text{HCl}(g)} &= 1.60 \times 10^{-3} + 6.0 \times 10^{-6}P - 1.594 \times 10^{-3}\text{Rel} \\ &\quad + 2.73 \times 10^{-4}\text{Rel}^2 - 1 \times 10^{-6}P \cdot \text{Rel} \end{aligned} \quad (22)$$

$$\begin{aligned} x_{\text{H}_2(g)} &= 2.048 \times 10^{-1} - 6.0 \times 10^{-6}P + 2.505 \times 10^{-1}\text{Rel} \\ &\quad + 2.0 \times 10^{-6}T - 2.6166 \times 10^{-2}\text{Rel}^2 \\ &\quad + 1.0 \times 10^{-6}P \cdot \text{Rel} \end{aligned} \quad (23)$$

where  $x_i$  is the molar concentration of specie  $i$  at equilibrium;  $P$  corresponds to the pressure (atm);  $T$  is the temperature (K); and Rel is the  $\text{H}_2/\text{SiCl}_4$  molar feed ratio.

The chlorosilanes produced are separated from the hydrogen and hydrogen chloride via condensation. The modeling of the condensation process is based on material and energy balances. Experimental results show complete separation of the condensed phase containing the chlorosilanes from the hydrogen and hydrogen chloride gas phase.<sup>23</sup>

**2.2.3. Separation and Purification.** The chlorosilanes are separated using conventional distillation. The process is carried out in a set of two conventional distillation columns. In the first column dome a  $\text{SiH}_2\text{Cl}_2\text{--SiHCl}_3$  mix is recovered, the composition of which depends on the operating conditions of the hydrochlorination reactor, while in the bottom of the column high purity  $\text{SiCl}_4$  (99.999% wt) is obtained. The second distillation column separates the  $\text{SiH}_2\text{Cl}_2\text{--SiHCl}_3$  mix to obtain high purity  $\text{SiH}_2\text{Cl}_2$  at the dome (99.999% wt), while from the bottom high purity  $\text{SiHCl}_3$  (99.999% wt) is recovered.<sup>9</sup>

On the basis of a previous work of Ramírez-Márquez et al.,<sup>27</sup> the distillation columns were rigorously modeled using Aspen Plus. To develop surrogate models for the chlorosilanes distillation, the product purity and size of the distillation columns were fixed in the simulations while the decision variables are the feed and the reflux ratios to compute the energy consumption and operating temperatures of each column. The ranges evaluated for these variables are the following:

- Feeding molar ratio (FR):  $\text{SiCl}_4\text{--}(\text{SiH}_2\text{Cl}_2\text{--SiHCl}_3)$  from 1 to 2.1698 for the first column;  $\text{SiH}_2\text{Cl}_2\text{--SiHCl}_3$  molar ratio from 2.99 to 7.5678 for the second column
- Reflux ratio (RR) from 10 to 80 for the first column and from 60 to 90 for the second column.

Surrogate models were developed considering the main variables affecting the distillation process, including the reboiler and condenser thermal duties, as well as the top and bottom temperatures, eqs 24 to 31.

$$\begin{aligned} Q_{\text{ConCol1}} &= -497.162 + 150.215\text{FR} - 495.071\text{RR} \\ &\quad - 2.17 \times 10^{-4}\text{RR}^2 + 150.191\text{FR} \cdot \text{RR} \end{aligned} \quad (24)$$

$$\begin{aligned} Q_{\text{RebCol1}} &= 909.868 - 209.970\text{FR} + 495.071\text{RR} \\ &\quad + 2.14 \times 10^{-4}\text{RR}^2 - 150.191\text{FR} \cdot \text{RR} \end{aligned} \quad (25)$$

$$\begin{aligned} T_{\text{ConCol1}} &= 351.296 - 4.93 \times 10^{-4}\text{RR} - 1.70050\text{FR} \\ &\quad + 6 \times 10^{-6}\text{RR}^2 - 1.0 \times 10^{-4}\text{RR} \cdot \text{FR} \end{aligned} \quad (26)$$

$$T_{\text{RebCol1}} = 387.695 - 9.0 \times 10^{-6}\text{FR} \quad (27)$$

$$\begin{aligned} Q_{\text{ConCol2}} &= -15.777 - 1.1074\text{FR} - 18.3726\text{RR} \\ &\quad + 1.0438 \times 10^{-1}\text{FR}^2 + 1.0 \times 10^{-6}\text{RR}^2 \\ &\quad + 3.632 \times 10^{-3}\text{FR} \cdot \text{RR} \end{aligned} \quad (28)$$

$$\begin{aligned} Q_{\text{RebCol2}} &= 19.968 + 9.4538\text{FR} + 18.3726\text{RR} \\ &\quad - 1.0427 \times 10^{-1}\text{FR}^2 - 1.0 \times 10^{-6}\text{RR}^2 \\ &\quad - 3.632 \times 10^{-3}\text{FR} \cdot \text{RR} \end{aligned} \quad (29)$$

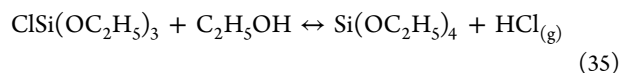
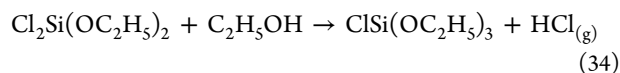
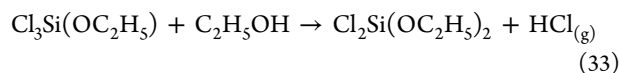
$$T_{\text{ConCol2}} = 321.8 - 1 \times 10^{-6}\text{FR} \quad (30)$$

$$T_{\text{RebCol2}} = 346.2 + 1.714\text{FR} - 1.057 \times 10^{-1}\text{FR}^2 \quad (31)$$

**2.2.4. RD Technology to Produce TEOS.** The work of Sánchez-Ramírez et al.,<sup>28</sup> shows the advantages of the intensified process based on reactive distillation (RD) by making a comparison with the traditional process using a reaction–separation scheme. The application of the RD technology to produce TEOS in a single unit seems to be an adequate alternative in order to produce high purity tetraethoxysilane. The aim to add this technology is to take advantage of the pure  $\text{SiCl}_4$  stream for the generation of a high added value product such as TEOS with different levels of purity (98.5–99.0–99.5).

The reactive distillation columns will be able to produce a wide range of TEOS purities in the same column simply by varying the operating variables. To develop a surrogate model for the columns the model developed in the work of Sánchez-Ramírez et al.,<sup>19</sup> is used where the design, the simulation, and the evaluation of the economic (ROI) and environmental (Eco

indicator 99) performance of these units was carried out. The chemical reaction sequence is represented in eqs 32 to 35.



In accordance with the work of the Sánchez-Ramírez et al.,<sup>19</sup> all reactive stages were considered under thermodynamic equilibrium. The Gibbs free energy minimization is used to model the species equilibrium. The need for accurate thermodynamic calculations involving enthalpy and entropy suggest the use of Aspen Plus to model the RD column covering a wide range of TEOS purities. Note that, analyzing the performance of the unit, the most important variables are the bottom flow rate and reboiler heat duty: as the bottom flow rate increases, smaller purity is obtained. Furthermore, as the reboiler duty decreases so does the product purity.

With the use of the Aspen Plus model developed in a previous work,<sup>27</sup> data on the operation of the RD column was collected for each TEOS purity. In this work a superstructure with the three products in parallel is developed. Due to the effect of the reboiler duty on the purity and the fact that different purities are fixed to define each product, the  $\text{SiCl}_4$  feed is the only important variable to consider in the model. The column design parameters must remain fixed to meet the required purity (input and output models). By varying the feed, the dome flows of the column at the bottom of the column were obtained, as well as the thermal load of the condenser and reboiler. The surrogate models for the reactive distillation column that produces each purity of TEOS are shown in the eqs 36 to 71. Each of the models presented below, describes the operating conditions of the column to produce each of these substances.

Surrogate model for the column that produces TEOS at 0.985:

- Component flow of dome stream:

$$f_{c(\text{SiCl}_4)} = f_{c_{\text{bottom of the column}(\text{SiCl}_4)}} \cdot 0.48053 \quad (36)$$

$$f_{c(\text{C}_2\text{H}_5\text{OH})} = f_{c_{\text{bottom of the column}(\text{SiCl}_4)}} \cdot 0.000383 \quad (37)$$

$$f_{c(\text{SiOC}_2\text{H}_5)} = f_{c_{\text{bottom of the column}(\text{SiCl}_4)}} \cdot 0.004923 \quad (38)$$

$$f_{c(\text{HCl})} = f_{c_{\text{bottom of the column}(\text{SiCl}_4)}} \cdot 2.06755 \quad (39)$$

$$f_{c(\text{N}_2)} = f_{c_{\text{bottom of the column}(\text{SiCl}_4)}} \cdot 2.3684 \quad (40)$$

- Component flow of bottom stream:

$$f_{c(\text{SiCl}_4)} = f_{c_{\text{bottom of the column}(\text{SiCl}_4)}} \cdot 0.00258 \quad (41)$$

$$f_{c(\text{C}_2\text{H}_5\text{OH})} = f_{c_{\text{bottom of the column}(\text{SiCl}_4)}} \cdot 0.00211 \quad (42)$$

$$f_{c(\text{SiOC}_2\text{H}_5)} = f_{c_{\text{bottom of the column}(\text{SiCl}_4)}} \cdot 0.51196 \quad (43)$$

$$f_{c(\text{HCl})} = 0 \quad (44)$$

$$f_{c(\text{N}_2)} = 0 \quad (45)$$

- For heat duty of the condenser and reboiler:

$$-Q_{\text{ConRDTEOS98,5}} = f_{c_{\text{bottom of the column}(\text{SiCl}_4)}} \cdot 78.85959 \quad (46)$$

$$Q_{\text{RebRDTEOS98,5}} = f_{c_{\text{bottom of the column}(\text{SiCl}_4)}} \cdot 63.3406 \quad (47)$$

Surrogate model for the column that produces TEOS at 0.99:

- Component flow of dome stream:

$$f_{c(\text{SiCl}_4)} = f_{c_{\text{bottom of the column}(\text{SiCl}_4)}} \cdot 0.478771924 \quad (48)$$

$$f_{c(\text{C}_2\text{H}_5\text{OH})} = f_{c_{\text{bottom of the column}(\text{SiCl}_4)}} \cdot 0.00065 \quad (49)$$

$$f_{c(\text{SiOC}_2\text{H}_5)} = f_{c_{\text{bottom of the column}(\text{SiCl}_4)}} \cdot 0.00918 \quad (50)$$

$$f_{c(\text{HCl})} = f_{c_{\text{bottom of the column}(\text{SiCl}_4)}} \cdot 2.06479 \quad (51)$$

$$f_{c(\text{N}_2)} = f_{c_{\text{bottom of the column}(\text{SiCl}_4)}} \cdot 2.36847 \quad (52)$$

- Component flow of bottom stream:

$$f_{c(\text{SiCl}_4)} = f_{c_{\text{bottom of the column}(\text{SiCl}_4)}} \cdot 0.00503 \quad (53)$$

$$f_{c(\text{C}_2\text{H}_5\text{OH})} = f_{c_{\text{bottom of the column}(\text{SiCl}_4)}} \cdot 0.00461 \quad (54)$$

$$f_{c(\text{SiOC}_2\text{H}_5)} = f_{c_{\text{bottom of the column}(\text{SiCl}_4)}} \cdot 0.50702 \quad (55)$$

$$f_{c(\text{HCl})} = 0 \quad (56)$$

$$f_{c(\text{N}_2)} = 0 \quad (57)$$

- For heat duty of the condenser and reboiler:

$$-Q_{\text{ConRDTEOS99,0}} = f_{c_{\text{bottom of the column}(\text{SiCl}_4)}} \cdot 65.52129 \quad (58)$$

$$Q_{\text{RebRDTEOS99,0}} = f_{c_{\text{bottom of the column}(\text{SiCl}_4)}} \cdot 49.56133 \quad (59)$$

Surrogate model for the column that produces TEOS at 0.995:

- Component flow of dome stream:

$$f_{c(\text{SiCl}_4)} = f_{c_{\text{bottom of the column}(\text{SiCl}_4)}} \cdot 0.47715 \quad (60)$$

$$f_{c(\text{C}_2\text{H}_5\text{OH})} = f_{c_{\text{bottom of the column}(\text{SiCl}_4)}} \cdot 0.00087 \quad (61)$$

$$f_{c(\text{SiOC}_2\text{H}_5)} = f_{c_{\text{bottom of the column}(\text{SiCl}_4)}} \cdot 0.01352 \quad (62)$$

$$f_{c(\text{HCl})} = f_{c_{\text{bottom of the column}(\text{SiCl}_4)}} \cdot 2.06185 \quad (63)$$

$$f_{c(\text{N}_2)} = f_{c_{\text{bottom of the column}(\text{SiCl}_4)}} \cdot 2.36848 \quad (64)$$

- Component flow of bottom stream:

$$f_{c(\text{SiCl}_4)} = f_{c_{\text{bottom of the column}(\text{SiCl}_4)}} \cdot 0.00738 \quad (65)$$

$$f_{c(\text{C}_2\text{H}_5\text{OH})} = f_{c_{\text{bottom of the column}(\text{SiCl}_4)}} \cdot 0.00733 \quad (66)$$

$$f_{c(\text{SiOC}_2\text{H}_5)} = f_{c_{\text{bottom of the column}(\text{SiCl}_4)}} \cdot 0.50194 \quad (67)$$

$$f_{c(\text{HCl})} = 0 \quad (68)$$

$$f_{c(\text{N}_2)} = 0 \quad (69)$$

- For heat duty of the condenser and reboiler:

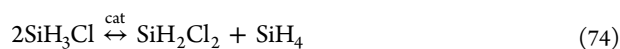
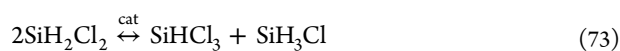
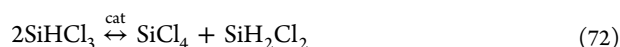
$$-Q_{\text{ConRDTEOS99,5}} = f_{c_{\text{bottom of the column}(\text{SiCl}_4)}} \cdot 61.69701 \quad (70)$$

$$Q_{\text{RebRDTEOS99,5}} = f_{c_{\text{bottom of the column}(\text{SiCl}_4)}} \cdot 45.31013 \quad (71)$$

where  $f_{c(x)}$  is the molar flow of each product in kmol/h;  $f_{c_{\text{bottom of the column}(\text{SiCl}_4)}}$  is the molar flow of  $\text{SiCl}_4$  coming from the separation in kmol/h;  $Q_{\text{ConRDTEOS}}$  is the condenser heat duty of the column; and  $Q_{\text{RebRDTEOS}}$  is the reboiler heat duty of the column (kJ/h).

**2.2.5. RD Technology to Produce Silane, Monochlorosilane, or Dichlorosilane.** The bottom stream of the distillation columns that process the mixture  $\text{SiH}_2\text{Cl}_2$ – $\text{SiHCl}_3$  contains  $\text{SiHCl}_3$  that will be divided to feed two processes: a reactive distillation column for the production of chlorosilanes and a set of Siemens reactors for the production of polycrystalline silicon. For the RD technology to produce  $\text{SiH}_4$ ,  $\text{SiH}_2\text{Cl}_2$ ,  $\text{SiH}_3\text{Cl}$ ,<sup>29</sup> a conceptual design of a single reactive distillation column is presented that produces a high purity of each of them. The relevance of the work<sup>29</sup> is that it shows the feasibility of producing pure  $\text{SiH}_4$ ,  $\text{SiH}_2\text{Cl}_2$ , or  $\text{SiH}_3\text{Cl}$  in the same RD column by simply varying the operating conditions. That work optimized the economics and environmental impact of the production of chlorosilanes. The column design considers the benefits of the intensification process, having as a target, besides the recovery of the three products independently, the reduction of the environmental impact. Composition, temperature, and cascading control structures were also developed in that work.

The reaction system consists of three simultaneous reactions. In the first one, trichlorosilane ( $\text{SiHCl}_3$ ) reacts to dichlorosilane ( $\text{SiH}_2\text{Cl}_2$ ) and tetrachlorosilane ( $\text{SiCl}_4$ ). Subsequently, dichlorosilane reacts to monochlorosilane ( $\text{SiH}_3\text{Cl}$ ) and trichlorosilane. Finally, monochlorosilane is converted to silane ( $\text{SiH}_4$ ) and dichlorosilane. The three reaction steps are shown in eqs 72 to 74.



The entire design of the multitasking reactive distillation column was generated using the Aspen Plus process simulator. As in the case of the previous RD column, by fixing the operating conditions that optimize the production of each one of the products, the feed of  $\text{SiHCl}_3$  allows computation of the dome and bottom flows of the column as well as the thermal duty of the condenser and reboiler. The input and output models for the RD column are shown in the eqs 75 to 110. Note that it is the same reactive distillation column that, when the operating conditions are changed, is capable of producing the three different products with high added value ( $\text{SiH}_4$ ,  $\text{SiH}_2\text{Cl}_2$ , and  $\text{SiH}_3\text{Cl}$ ).

#### 1st Operating mode: production of $\text{SiH}_4$ .

- Component flow of from the top:

$$f_{c_{(\text{SiHCl}_3)}} = 0 \quad (75)$$

$$f_{c_{(\text{SiCl}_4)}} = 0 \quad (76)$$

$$f_{c_{(\text{SiH}_2\text{Cl}_2)}} = 0 \quad (77)$$

$$f_{c_{(\text{SiH}_4)}} = f_{c_{\text{split}(\text{SiHCl}_3)}} \cdot 2.46 \times 10^{-1} \quad (78)$$

$$f_{c_{(\text{SiH}_3\text{Cl})}} = f_{c_{\text{split}(\text{SiHCl}_3)}} \cdot 3.75 \times 10^{-3} \quad (79)$$

- Component flow from the bottoms:

$$f_{c_{(\text{SiHCl}_3)}} = f_{c_{\text{split}(\text{SiHCl}_3)}} \cdot 0.0037529 \quad (80)$$

$$f_{c_{(\text{SiCl}_4)}} = f_{c_{\text{split}(\text{SiHCl}_3)}} \cdot 0.74625 \quad (81)$$

$$f_{c_{(\text{SiH}_2\text{Cl}_2)}} = 0 \quad (82)$$

$$f_{c_{(\text{SiH}_4)}} = f_{c_{\text{split}(\text{SiHCl}_3)}} \cdot 0 \quad (83)$$

$$f_{c_{(\text{SiH}_3\text{Cl})}} = 0 \quad (84)$$

- For heat duty of the condenser and reboiler:

$$-Q_{\text{ConRDSiH}_4} = f_{c_{\text{split}(\text{SiHCl}_3)}} \cdot 55.68329 \quad (85)$$

$$Q_{\text{RebRDSiH}_4} = f_{c_{\text{split}(\text{SiHCl}_3)}} \cdot 58.84151 \quad (86)$$

#### 2nd Operating mode: production of $\text{SiH}_2\text{Cl}_2$ .

- Component flow of from the top:

$$f_{c_{(\text{SiHCl}_3)}} = f_{c_{\text{split}(\text{SiHCl}_3)}} \cdot 0.00376 \quad (87)$$

$$f_{c_{(\text{SiCl}_4)}} = 0 \quad (88)$$

$$f_{c_{(\text{SiH}_2\text{Cl}_2)}} = f_{c_{\text{split}(\text{SiHCl}_3)}} \cdot 0.49249 \quad (89)$$

$$f_{c_{(\text{SiH}_4)}} = 0 \quad (90)$$

$$f_{c_{(\text{SiH}_3\text{Cl})}} = f_{c_{\text{split}(\text{SiHCl}_3)}} \cdot 0.00374 \quad (91)$$

- Component flow from the bottoms:

$$f_{c_{(\text{SiHCl}_3)}} = f_{c_{\text{split}(\text{SiHCl}_3)}} \cdot 1.44911 \times 10^{-5} \quad (92)$$

$$f_{c_{(\text{SiCl}_4)}} = f_{c_{\text{split}(\text{SiHCl}_3)}} \cdot 0.49998 \quad (93)$$

$$f_{c_{(\text{SiH}_2\text{Cl}_2)}} = 0 \quad (94)$$

$$f_{c_{(\text{SiH}_4)}} = f_{c_{\text{split}(\text{SiHCl}_3)}} \cdot 0 \quad (95)$$

$$f_{c_{(\text{SiH}_3\text{Cl})}} = 0 \quad (96)$$

- For heat duty of the condenser and reboiler ( $\text{SiH}_2\text{Cl}_2$ ):

$$-Q_{\text{ConRDSiH}_2\text{Cl}_2} = f_{c_{\text{split}(\text{SiHCl}_3)}} \cdot 82.37442 \quad (97)$$

$$Q_{\text{RebRDSiH}_2\text{Cl}_2} = f_{c_{\text{split}(\text{SiHCl}_3)}} \cdot 84.24849 \quad (98)$$

#### 3rd Operating mode: production of $\text{SiH}_3\text{Cl}$ .

- Component flow of from the top:

$$f_{c_{(\text{SiHCl}_3)}} = 0 \quad (99)$$

$$f_{c_{(\text{SiCl}_4)}} = 0 \quad (100)$$

$$f_{c_{(\text{SiH}_2\text{Cl}_2)}} = f_{c_{\text{split}(\text{SiHCl}_3)}} \cdot 2.93 \times 10^{-3} \quad (101)$$

$$f_{c(\text{SiH}_4)} = f_{c_{\text{split}(\text{SiHCl}_3)}} \cdot 2.07 \times 10^{-3} \quad (102)$$

$$f_{c(\text{SiH}_3\text{Cl})} = f_{c_{\text{split}(\text{SiHCl}_3)}} \cdot 3.28 \times 10^{-1} \quad (103)$$

$$f_{c(\text{SiHCl}_3)} = f_{c_{\text{split}(\text{SiHCl}_3)}} \cdot 0.00035 \quad (104)$$

$$f_{c(\text{SiCl}_4)} = f_{c_{\text{split}(\text{SiHCl}_3)}} \cdot 0.6661471 \quad (105)$$

- Component flow from the bottoms:

$$f_{c(\text{SiH}_2\text{Cl}_2)} = 0 \quad (106)$$

$$f_{c(\text{SiH}_4)} = 0 \quad (107)$$

$$f_{c(\text{SiH}_3\text{Cl})} = 0 \quad (108)$$

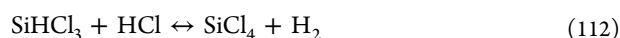
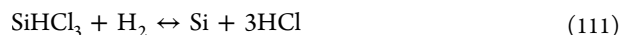
- For heat duty of the condenser and reboiler:

$$-Q_{\text{ConRDSiH}_3\text{Cl}} = f_{c_{\text{split}(\text{SiHCl}_3)}} \cdot 45.15792 \quad (109)$$

$$Q_{\text{RebRDSiH}_3\text{Cl}} = f_{c_{\text{split}(\text{SiHCl}_3)}} \cdot 47.80694 \quad (110)$$

where  $f_{c(x)}$  is the molar flow of each product in kmol/h;  $f_{c_{\text{split}(\text{SiHCl}_3)}}$  is the molar flow of  $\text{SiHCl}_3$  coming from the split in kmol/h;  $Q_{\text{ConRD}}$  is the condenser heat duty of the column; and  $Q_{\text{RebRD}}$  is the reboiler heat duty of the column (kJ/h).

**2.2.6. Siemens Reactor.** The production of polycrystalline silicon is performed in a Siemens reactor, where the polysilicon is deposited on ultrapure silicon electrically heated rods. During the deposition process, which takes from 3 to 5 days, the rods grow continuously until reaching a thickness of 80 mm–150 mm per rod.<sup>30</sup> As a consequence of the batch nature of the polysilicon deposition, it is necessary to use several deposition reactors operating in parallel with complementary scheduling schemes to reach the required production. Since the production of each Siemens reactor unit is 11.77 kg/h,<sup>30</sup> to reach a total production of 15 000 ton/y, 150 Siemens reactor units are required to complete the production. The reactions are showed in eqs 111 and 112.<sup>31</sup>



The reactor was modeled according to the work by Del Coso and Luque.<sup>31</sup> To model the polysilicon deposition, the second-order reaction is split in two reaction systems of first-order. The main variables of the deposition process include growth rate, deposition efficiency, and power-loss that are a function of the gas velocity, the composition of the feed, the reactor pressure, and the surface temperature. The production of polycrystalline silicon is computed providing information regarding the deposition velocity.

However, since the model described by Del Coso and Luque<sup>31</sup> is too complex to be included in the superstructure optimization problem, a surrogate model is developed to estimate the species distribution as a function of the temperature within the range studied, eqs 113–116. It should be noted that the reaction coefficients estimated for the eqs 111 and 112 are validated at atmospheric pressure. Consequently, the surrogate model is not able to consider the effect of pressure inside the reactor for values different to atmospheric pressure.

$$X_{\text{Si}(s)} = -6.220 \times 10^{-7} T^2 + 1.8580059 \times 10^{-3} T - 1.3159371763 \quad (113)$$

$$X_{\text{H}_2(g)} = 3.9 \times 10^{-9} T^2 - 1.17934 \times 10^{-5} T + 1.47006954 \times 10^{-2} \quad (114)$$

$$X_{\text{HCl}(g)} = 3.57 \times 10^{-8} T^2 - 1.066805 \times 10^{-4} T + 1.329638743 \times 10^{-1} \quad (115)$$

$$X_{\text{SiCl}_4(g)} = 1 - X_{\text{Si}(s)} - X_{\text{H}_2(g)} - X_{\text{HCl}(g)} \quad (116)$$

The variables in eqs 113–116 are the following:  $X_i$  is the concentration of the species  $i$  (mass fraction) and  $T$  is the temperature (K). The polycrystalline silicon deposition is the largest contributor to the energy consumption of the overall process, resulting in an electrical consumption of 60 kWh per kg.<sup>30</sup> Exchangers and separation tanks are used to recover the solar grade polysilicon and gases. These were modeled by energy and mass balances. The validation of the surrogate models obtained for each unit can be found in the [Supporting Information](#). It can be noticed that the surrogate model reproduces accurately the detailed simulation or experimental data.

**2.2.7. Auxiliary Equipment.** All auxiliary equipment such as separators, heat exchangers, and pumps were modeled according to mass and energy balances in the steady state. Concerning compressor modeling, polytrophic behavior for all compressors was considered, as well as an efficiency,  $n_c$ , of 0.85.<sup>32</sup> The polytrophic coefficient,  $z$ , was obtained from Aspen Plus offline simulations, and has a value of 1.4. The energy balance for the compressors was estimated considering eqs 117 and 118.

$$T_{\text{out compressor}} = T_{\text{in compressor}} + T_{\text{in compressor}} \left( \left( \frac{P_{\text{out compressor}}}{P_{\text{in compressor}}} \right)^{z-1/z} - 1 \right) \frac{1}{n_c} \quad (117)$$

$$W_{(\text{compressor})} = F \left( \frac{Rz(T_{\text{in compressor}})}{((M_w)(z-1))} \right) \frac{1}{n_c} \left( \left( \frac{P_{\text{out compressor}}}{P_{\text{in compressor}}} \right)^{z-1/z} - 1 \right) \quad (118)$$

where  $T_{\text{out compressor}}$  is the out temperature (K);  $T_{\text{in compressor}}$  is the entry temperature (K);  $P_{\text{out compressor}}$  is the out pressure (kPa);  $P_{\text{in compressor}}$  is the entry pressure (kPa);  $z$  is a polytrophic coefficient;  $n_c$  is the efficiency of the compressor;  $W_{(\text{compressor})}$  is the electrical energy (kW); and  $R$  is the constant of ideal gases in SI units.

**2.3. Solution Procedure.** The process was formulated as a nonlinear programming (NLP) problem. The model consists of 3014 equations and 3716 variables, which are solved to optimize the operating conditions of the multiproduct polycrystalline silicon facility, using a simplified profit objective function, eq 119. The superstructure includes three reactive distillation columns in parallel for the production of the three TEOS purities, as well as three other reactive distillation columns in parallel for each of the chlorosilanes. Hence, the main decision variables are the temperature of the thermal carboreduction reactor; the temperature, pressure, and  $\text{H}_2/\text{SiCl}_4$  feeding molar ratio of the hydrochlorination reactor, the

feeding ratio and the reflux ratio of each distillation column, for the reactive columns the feeding ratio, and the operating temperature of the Siemens Reactor.

The objective function, eq 119, aims to maximize the process total profit, considering not only the production of the main product (polysilicon), but also the income from byproducts (chlorosilanes), deducting the manufacturing cost.

$$(OF)\max z = S_{\text{polycrystalline silicon}} + pSP - bRM - cE \quad (119)$$

where  $b$  is the unit cost of each raw material RM;  $c$  is the cost of each utility  $E$ ;  $p$  is the price of each byproduct SP, and  $S_{\text{polycrystalline silicon}}$  is profit from the sale of the polycrystalline silicon.

Also, a detailed economic evaluation based on the procedure proposed by Turton et al.<sup>33</sup> was carried out, estimating the equipment cost, production cost, maintenance, administration, and manpower. The NLP problem was solved using a multistart initialization approach with CONOPT as the preferred solver.

### 3. RESULTS

Initially the optimization of the model corresponding to the polycrystalline silicon plant and other products of high added value (TEOS at different purities, silane, dichlorosilane, and monochlorosilane), was considered with a single scenario. This scenario is to maximize the economic profit of the process and thus be able to reduce the cost of polycrystalline silicon. It is important to mention that in this scenario, all the variables (temperature, pressure, feed ratios, reactive distillation column feed, etc.) were left free, in order to find an optimal profit and portfolio of products. During the optimization under this scenario (S1) and to guarantee the maximum economic profit of the process, it was observed that the model tends to produce polycrystalline silicon, silane, dichlorosilane (generated at the hydrochlorination reactor) and TEOS 99.5 (see Table 2), thus

**Table 2. Profit [M\$/y], Operating Costs [M\$/y], kg of Polycrystalline Silicon/h, kg of TEOS, and kg of Silane of the Objective Function**

| multiproduct polycrystalline silicon facility | S1       | S2      | S3      | S4      |
|---|----------|---------|---------|---------|
| profit [M\$/y]                                | 117.94   | 110.07  | 114.09  | 110.36  |
| operating costs [M\$/y]                       | 16.09    | 14.01   | 15.25   | 14.05   |
| kg of polycrystalline silicon/h               | 1875     | 1708    | 1768    | 1656    |
| kg of TEOS (99.5 of purity)/h                 | 26.91    | 0       | 0       | 22.54   |
| kg of TEOS (99.0 of purity)/h                 | 0        | 22.09   | 0       | 20.22   |
| kg of TEOS (98.5 of purity)/h                 | 0        | 0       | 147.69  | 20.34   |
| kg of SiH <sub>4</sub> /h                     | 4.595    | 8.73    | 7.902   | 9.926   |
| kg of SiH <sub>2</sub> Cl <sub>2</sub> /h     | 2668.694 | 2656.65 | 1667.59 | 2701.57 |
| kg of SiH <sub>3</sub> Cl/h                   | 0        | 0       | 0       | 164.11  |

not considering the production of other value-added products such as TEOS 99.0, TEOS 98.5, and monochlorosilane. This solution is somehow expected since, while aiming at maximum profit, the species with the highest price are selected. Note that the global optimum is not claimed.

Apart from the optimization targeting economic profit, S1, another three scenarios were also evaluated. The second

scenario (S2), guarantees the production of TEOS 99.0 instead of any other purity and any of the chlorosilanes. The same objective function given by eq 119 is used. This scenario was specified by providing a lower bound for the production of SiCl<sub>4</sub> of 10 kmol/h to the reactive distillation column for the production of TEOS 99.0, and zero for the other two purities of TEOS. In the case of the production of chlorosilanes, the algorithm for the selection of some of the chlorosilanes or, alternatively, the choice of polycrystalline silicon was left free. In a third scenario (S3), the process is intended to produce TEOS 98.5 and some of the chlorosilanes, which guarantees maximum process profit under these circumstances. In the third scenario, a lower bound for the production of TEOS 98.5 is considered by assuming a feed to the reactive distillation column that produces at least 10 kmol/h (for the other two TEOS purities, the model was forced to stop feeding the RD columns); and the flow of the stream of SiHCl<sub>3</sub> for the production of chlorosilanes or polycrystalline silicon is free. The fourth scenario (S4) requires the process to produce all products with high added value, also guaranteeing a maximum profit. For this last scenario, all TEOS purities are to be produced in the same proportion. Thus, lower bounds to the feeds of SiCl<sub>4</sub> to each reactive distillation column for the production of TEOS are provided. Likewise, the stream containing high purity SiHCl<sub>3</sub> was forced to split and at least feed an amount of trichlorosilane to the multitasking reactive distillation column of chlorosilanes in each of the operating conditions, so that it was capable of producing all three, SiH<sub>4</sub>, SiH<sub>2</sub>Cl<sub>2</sub>, and SiH<sub>3</sub>Cl. Note that in each of the scenarios proposed, the operating conditions of each unit will vary, and therefore the energy and economic costs of the process will vary as well. To achieve the production capacity of typical industrial plants of 15 000 ton/y, in the present work a feed of 120 kmol/h of SiO<sub>2</sub> and 240 kmol/h of C is considered in each scenario.

It is important to mention that the number of scenarios can be infinity considering all combinations of the products that can be produced, that is, a certain amount of TEOS at various purities and chlorosilanes. With the proposed scenarios, it is expected to present the big picture of the process both in profit, as in the final costs of polycrystalline silicon. That is why the choice of feeds to reactive distillation columns, both for the production of TEOS and chlorosilanes, could take higher or lower values. Here the aim was to investigate was the effect of producing such components.

In Table 2, the flows of the portfolio of selected products under each of the scenarios are presented. As it is expected, under S1 the process obtains its maximum profit (117.94 M \$/y), in addition it can be observed that this is the scenario with the largest production of polycrystalline silicon, resulting in a total of 15 938 ton/y. Scenario S2 produces polycrystalline silicon, TEOS 99.0, dichlorosilane from the hydrochlorination reactor, and silane. In this scenario, the total profit is reduced by 6.67%, because the production of polycrystalline silicon is reduced by 9% since the process seeks to produce other value-added products such as silane and TEOS 99.0, which are of lower value compared to the products obtained in the previous scenario. This is because the model chooses to produce almost double the silane in S2 compared to S1, which reduces the feed of trichlorosilane to the deposition reactors, and therefore reduces the production of polycrystalline silicon. Something similar occurs with scenarios 3 and 4 (S3 and S4), where the process profit is lower than that in S1. In the case of S3, the

profit is larger than for S2 and S4, because the production of polycrystalline silicon is higher than in the other scenarios. For S4 all possible products in the plant are obtained. The profit of this last scenario decreases by 6.42%, resulting in a decrease in the sale price of polycrystalline silicon of 2.33% with respect to S1, see Table 3.

**Table 3. Price of Each Product for All Scenarios**

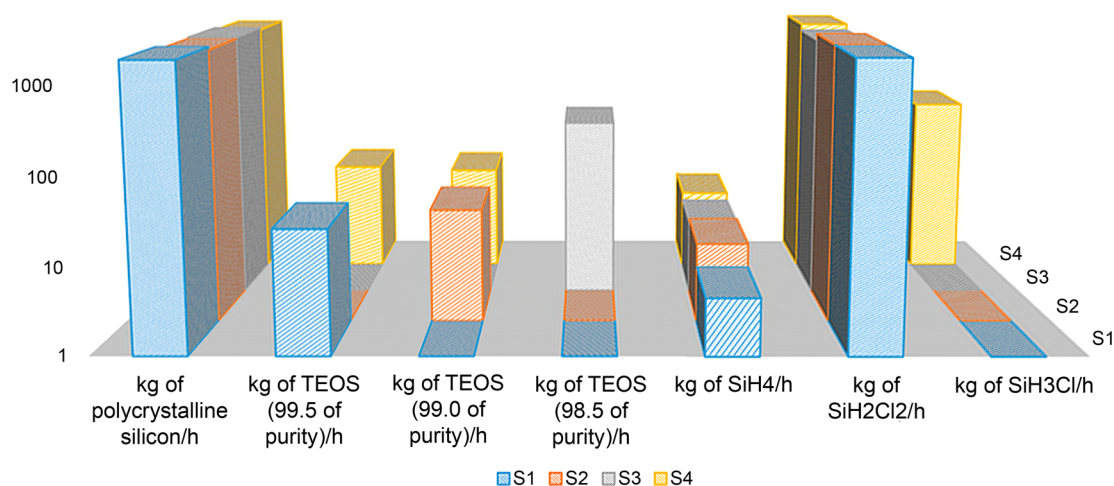
| price   | S1   | S2                  | S3   | S4   |
|---|------|---------------------|------|------|
| polycrystalline silicon \$/kg                   | 6.86 | 6.99                | 7.23 | 7.02 |
| TEOS 99.5 \$/kg                                 |      | 3.75 <sup>34</sup>  |      |      |
| TEOS 99.0 \$/kg                                 |      | 2.50 <sup>35</sup>  |      |      |
| TEOS 98.5 \$/kg                                 |      | 1.50 <sup>36</sup>  |      |      |
| SiH <sub>4</sub> \$/kg                          |      | 88.44 <sup>37</sup> |      |      |
| price of SiH <sub>2</sub> Cl <sub>2</sub> \$/kg |      | 3.67 <sup>38</sup>  |      |      |
| SiH <sub>3</sub> Cl \$/kg                       |      | 3.0 <sup>39</sup>   |      |      |

Figure 2 shows the product portfolio of the different scenarios. It is clear that the production rate of polycrystalline silicon, and that of each of the high value-added products determines the final profit and the production cost of polycrystalline silicon.

**3.1. Main Operating Parameters.** The main operating conditions in the facility are summarized in Table 4; where the operating temperature and pressure of each of the major equipment pieces for the production of polycrystalline silicon and several byproducts with high added value is presented. It can be seen that the temperature and pressure of the main units change when the demand for polycrystalline silicon also changes. In the carboreduction reactor it is observed that the larger is the production of polycrystalline silicon, the larger is the required production of metallurgical silicon; therefore the temperature of the carboreduction reactor is adjusted for the production of metallurgical silicon depending on the scenario. The highest profit results in the lowest operating temperature at the carboreduction unit. This translates into a metallurgical silicon production capacity in the range of 1400–1600 kg/h for the carboreduction reactor for the four scenarios. In this range, the conditions of the carboreduction reactor are adjusted within the range presented in section 2.2.1, to produce the flow of metallurgical silicon necessary for the chlorosilane production process in the hydrochlorination

reactor. In the case of the hydrochlorination reactors, the operating conditions are within the temperature range of 673–680 K, an operating pressure of 2026 kPa and a feed ratio of H<sub>2</sub>/SiCl<sub>4</sub> between 1.91 and 5. Lower feed ratio and temperatures are selected to achieve a larger profit where the pressure is almost constant in all cases. This is to guarantee the adequate chlorosilanes production (SiHCl<sub>3</sub>, SiH<sub>2</sub>Cl<sub>2</sub>, SiCl<sub>4</sub>) in each scenario (particularly trichlorosilane being the precursor of polycrystalline silicon). In all scenarios (conventional distillation columns and reactive distillation columns) the variables such as column height and the operating pressure in the installation remain constant across the different capacities. The variables such as the feeding ratio and, in the case of conventional columns, the reflux ratio are those that suffer variations in the process. These conditions can be observed in Table 4. For the conventional columns reflux ratio values from 13.93 to 80, for the SiHCl<sub>3</sub>–SiH<sub>2</sub>Cl<sub>2</sub>–SiCl<sub>4</sub> separation columns, and from 60 to 90 in the SiHCl<sub>3</sub>–SiH<sub>2</sub>Cl<sub>2</sub> separation columns are found. The temperature conditions of the Siemens reactors range from 1457 to 1500 K, ensuring maximum yield in each scenario.

In particular, it is observed that for S1, the temperature of the carboreduction reactor, 2819 K, is at the point of maximum production of metallurgical silicon which, in synchrony with the conditions of the hydrochlorination reactor with a temperature of 673 K and a pressure of 2026 kPa, guarantee a high production of trichlorosilane and a not-so-high production of SiH<sub>4</sub> and SiH<sub>2</sub>Cl<sub>2</sub>. This combination secures a high production of polycrystalline silicon and/or chlorosilanes, which therefore makes the process more profitable. Therefore, a reflux ratio around 15 is required in the set of the first conventional columns (where SiCl<sub>4</sub> is separated), and a high reflux ratio value (60.26) is suggested for the second set of conventional columns. This high value is required to guarantee the adequate separation and high purity of trichlorosilane. At the RD columns for the production of TEOS, the reflux ratio is small, 1.21. This value is consistent with the production of silane reported by Ramírez Márquez.<sup>27</sup> Regarding the deposition reactors, the temperature of 1500 K is the highest reported among all scenarios, and it is consistent with the highest production of polycrystalline silicon achieved in this scenario.



**Figure 2.** Production of polycrystalline silicon and each one of the products of high added value in each proposed scenario.



Table 5. Energy Requirements and Temperatures of Each Scenario<sup>a</sup>

|    | TCa    |         | separation                              |   | Col RD TEOS                             |   |   | Col RD SiH <sub>4</sub> - SiH <sub>2</sub> Cl <sub>2</sub> - SiH <sub>3</sub> Cl |   |   | Siemens |
|----|--------|---------|---|---|---|---|---|--|---|---|---------|
|    | Q [kW] | Hy [kW] | C1                                      | C 2                                     | 98.5                                    | 99.0                                    | 99.5                                    | SiH <sub>4</sub>   | SiH <sub>2</sub> Cl <sub>2</sub>        | SiH <sub>3</sub> Cl                     | Q [kW]  |
|    | Q [kW] | Q [kW]  | Q <sub>Con</sub> /Q <sub>Reb</sub> [kW] | Q <sub>Con</sub> /Q <sub>Reb</sub> [kW] | Q <sub>Con</sub> /Q <sub>Reb</sub> [kW] | Q <sub>Con</sub> /Q <sub>Reb</sub> [kW] | Q <sub>Con</sub> /Q <sub>Reb</sub> [kW] | Q <sub>Con</sub> /Q <sub>Reb</sub> [kW]  | Q <sub>Con</sub> /Q <sub>Reb</sub> [kW] | Q <sub>Con</sub> /Q <sub>Reb</sub> [kW] | Q [kW]  |
| S1 | 33279  | 4455    | -59720/60882                            | -6085/6284                              | N/A                                     | N/A                                     | -638/468                                | -252/266   | N/A                                     | N/A                                     | 108934  |
| S2 | 33157  | 4470    | -10912/12044                            | -5147/5392                              | N/A                                     | -32/25                                  | N/A                                     | -123/130   | N/A                                     | N/A                                     | 100480  |
| S3 | 42104  | 6049    | -10828/11987                            | -4480/4680                              | 258/208                                 | N/A                                     | N/A                                     | -111/117   | N/A                                     | N/A                                     | 106079  |
| S4 | 32754  | 4341    | -54800/55952                            | -6676/6924                              | -35/29                                  | -29/23                                  | -31/24                                  | -140./148  | -338/345                                | -679/718                                | 99580   |

<sup>a</sup>Notation: Comp = compressors; Exch = exchanger; St = steam; Co = coolant; Q = heat duty; Con = condenser; Reb = reboiler; W = work; N/A = not applicable.

conventional columns. This is due to the large amount of trichlorosilane that these two scenarios are required to produce chlorosilanes and polycrystalline silicon. The S2 presents a balance between the energy requirements and the quantity of products produced, being the third best scenario in polycrystalline silicon production, but increasing silane production. In S4 a smaller amount of energy is required at the deposition reactors, this is clearly observed by having a smaller amount of polycrystalline silicon produced.

**3.2. Polycrystalline Silicon Refinery and Other Value-Added Products Cost.** Numerous studies in the literature evaluate the effect of expected future investment costs for industrial processes.<sup>40,41</sup> In the case of the polycrystalline silicon refining plant and other products with high added value, the plant consists of a variety of equipment, such as the carboreduction reactor, the hydrochlorination reactors, and separation equipment (conventional distillation columns), reaction-separation equipment (reactive distillation columns), Siemens deposition reactors, compressors, tanks, exchangers, etc. The process described in Figure 1 shows a basic scheme for the positioning of each of the equipment and the function that it performs. In some cases more than one unit is required to meet the intended capacity. In this section the costs per equipment of the facility are estimated assuming that the process is flexible to change the portfolio of products. For that, the largest unit of any of the scenarios is sized and its cost is estimated.

In the case of carboreduction, only one reactor is sufficient to meet the requirement; in the chlorosilane production section, four reactors are required. Each of these units also requires a set of separation columns, with a total of eight conventional distillation columns. For high value-added compounds such as TEOS 99.5, TEOS 99.0, TEOS 98.5, silane, dichlorosilane, and monochlorosilane, reactive distillation columns are required independently. For each of the cases, that is TEOS or chlorosilanes, the columns multitask, and for each case with a single column of reactive distillation at different operating conditions, the different products are obtained. In the case of each reactive distillation column for TEOS and for chlorosilanes to ensure adequate production, a pair of reactive distillation columns are required (i.e., two RD columns for the production of TEOS at different purities, and a pair of RD columns for chlorosilanes). In the case of silicon deposition, 150 Siemens reactors are required to guarantee a production of around 15 000 ton/y. Table 6 shows the costs obtained from each unit, reaching a total costs of equipment of 85.83 M\$ for all scenarios (the same costs per equipment is used in all scenarios, since the cost of the equipment was made considering the maximum production of each product).

Table 6. Costs per Equipment Based on the Procedure Proposed by Turton et al.<sup>a,33</sup>

| equipment                      | number of units | total cost (\$) | total annualized cost (\$/y) |
|--------------------------------|-----------------|-----------------|------------------------------|
| tanks                          | 8               | \$360,307.62    | \$72,061.52                  |
| mixers                         | 6               | \$1,923,436.73  | \$384,687.35                 |
| thermal carboreduction reactor | 1               | \$11,462,274.00 | \$2,292,454.80               |
| melting pot                    | 1               | \$630,390.79    | \$126,078.16                 |
| conveyor belt                  | 1               | \$2,541,800.00  | \$508,360.00                 |
| hydrochlorination reactor      | 4               | \$1,591,515.82  | \$318,303.16                 |
| chlorosilanes separator        | 4               | \$898,288.64    | \$179,657.73                 |
| compressors                    | 14              | \$6,962,313.87  | \$1,392,462.77               |
| heat exchanger                 | 16              | \$1,827,836.81  | \$365,567.36                 |
| distillation columns           | 8               | \$16,695,330.43 | \$3,339,066.09               |
| RD column TEOS                 | 2               | \$10,730,435.20 | \$2,146,087.04               |
| RD column chlorosilanes        | 2               | \$6,444,144.76  | \$1,288,828.95               |
| Siemens reactor                | 150             | \$23,864,538.67 | \$4,772,907.73               |
| total                          |                 | \$85,932,613.34 | \$17,186,522.67              |

<sup>a</sup>5 years for the annualization.

The operating costs are also computed, and the evaluation is based on the procedure proposed by Turton et al.<sup>33</sup> Figure 3 shows conclusively the variation in the production costs depending on the scenario. It is evident that S1 shows higher production costs related to the raw material with respect to the other items such as electricity, steam, and refrigerants. This fact is linked to the fact that it corresponds to the scenario with the highest production of polycrystalline silicon. S3 shows the higher energy and refrigerant consumption than for the other scenarios. In general, it can be observed that in each scenario the costs of each of the items are balanced to guarantee maximum economic profit. In scenarios S2 and S4, a trade-off between raw material costs and refrigerant costs can be observed, they also have electricity costs in intermediate values with respect to the other two scenarios. In the specific case of S4, vapor cost values are increased due to the use of several distillation columns, both conventional and reactive.

**3.3. Estimated Price of Polycrystalline Silicon.** The average polycrystalline silicon price dropped below the 10 \$/kg threshold for the first time in 2019, according to PVInsights.<sup>42</sup> The analysis in this work shows that the polycrystalline silicon refining industry with other high value-added products might lower their production costs to 6.86 \$/kg polycrystalline silicon, a historical threshold, and still, prices could drop again if the range of high added value products is extended.

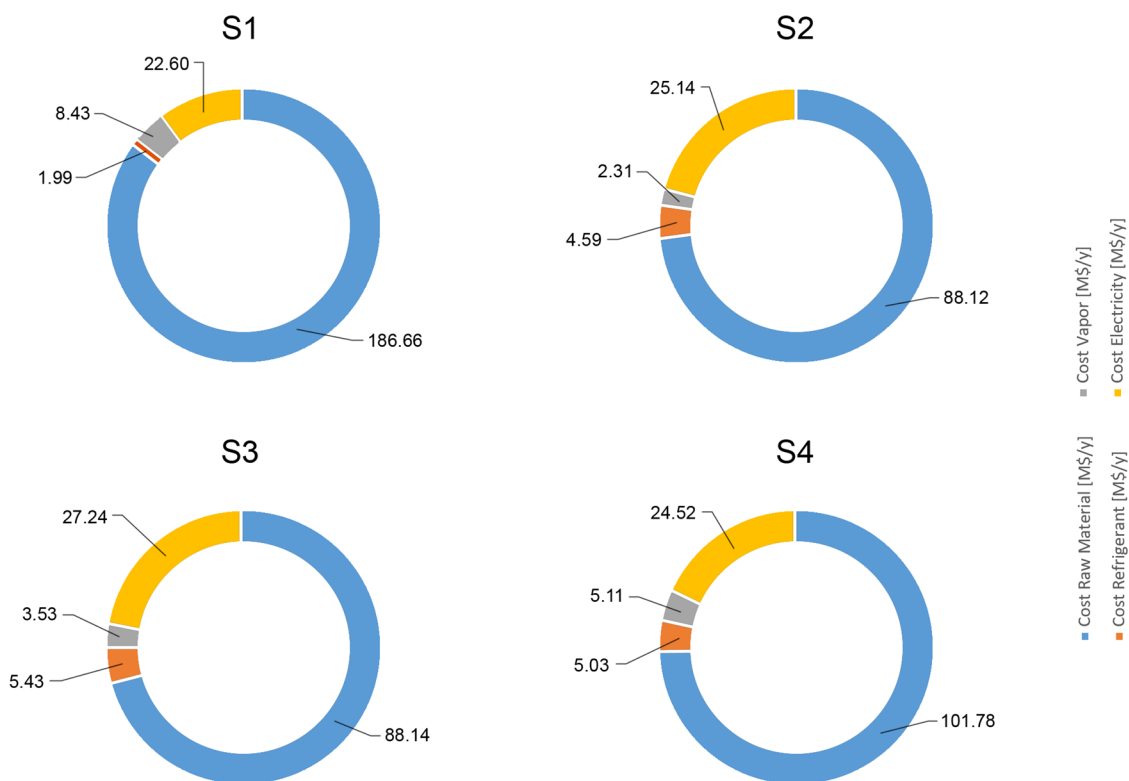


Figure 3. Costs of raw material, electricity, steam, and refrigerant for each scenario.

Figure 4 shows the variability of the price of polycrystalline silicon according to the proposed scenarios. In addition, the

Price of Polycrystalline Silicon \$/kg

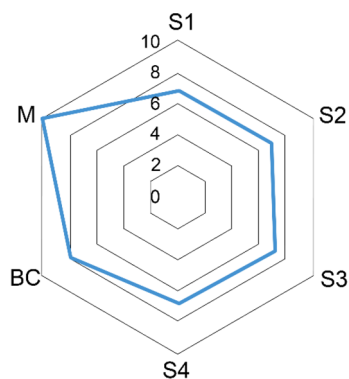


Figure 4. Estimated price of polycrystalline silicon in each scenario, without the generation of products with high added value (base case [BC]), and the market price according to PVInsights (M).<sup>42</sup>

cost of the polycrystalline silicon process if no additional high added value products were generated is also included as a base case (BC). It can be seen that in the four scenarios, the cost of polycrystalline silicon is considerably reduced with respect to the current market price of the case of single product process due to production of high value-added products. In Figure 4 it can also be seen that the vertices of scenarios 1 and 2 with respect to polycrystalline silicon costs are worse than in the others scenarios. This indicates that the simultaneous generation of high value-added products such as silane and TEOS at high purities (99.5 and 99.0) and polycrystalline silicon, leads to a substantial reduction in the cost of selling

polycrystalline silicon. And finally, the best scenario (S1) is capable of reducing the price of silicon by 17.64% compared to the production of polycrystalline silicon alone. There is also a 31.40% (S1) reduction with respect to the market sale price of polycrystalline silicon. Note that neither the gas treatment nor further processing after the production of rods are considered. However, it is clear that the production of byproducts reduces the production cost.

It should be noted that the macro-level relative demands for the polycrystalline silicon for the process for the multiproduct polycrystalline silicon refinery, meets the production capacity similar to the current polycrystalline silicon production companies such as Wacker Co., an average production capacity of 15 000 annual metric tons of polycrystalline silicon is considered.<sup>8</sup> Regarding the production of TEOS (with different purities), it should be mentioned that the TEOS market is relatively fragmented. A number of manufacturers of different scales are focusing on this market. The lack of raw materials and limited applications used to be the obstacles in this industry. Thus, only limited companies are able to produce high purity TEOS by their own technology. For the moment, the market of TEOS is quite competitive. Regionally, China is the biggest production base of TEOS, and the market share of EU is also considerable. Producers in the USA are less, but with a leading market share in the global market. As a kind of unconventional material, the production of TEOS highly depends on the downstream demand. Silicone rubber is the biggest market of TEOS, which took more than 25% (1000 ton/y) of total TEOS production in the last year.<sup>43</sup> With this work, the demand for TEOS for the silicone rubber market is expected to at least be met, with manufacturers being able to produce more than 1000 ton/y (98.5 of purity), compared to the requirement for the silicone rubber process. Likewise, the chlorosilanes ( $\text{SiH}_4$ ,  $\text{SiH}_2\text{Cl}_2$ ,  $\text{SiH}_3\text{Cl}$ ) market is dominated by

the Asia Pacific region, as China is the major producer and consumer of chlorosilanes. The electronics industry is growing significantly in China and India. The scenario is anticipated to be similar during the forecast period due to the growing electronics industry in the region. There are limitations in the production of the polycrystalline silicon and other high added value products related with the feeding of trichlorosilane to the reactive distillation column. However, the process is capable of producing 85 [ton/y] of  $\text{SiH}_4$ , 23 000 [ton/y] of  $\text{SiH}_2\text{Cl}_2$ , and 1400 [ton/y] of  $\text{SiH}_3\text{Cl}$ , in some scenarios. The above offers a comprehensive demand of the chlorosilanes market.<sup>44</sup>

#### 4. CONCLUSIONS

In this work a superstructure optimization approach is used for the selection of the portfolio of products within a multiproduct polycrystalline silicon facility. Surrogate models for major units allow selecting the yield and operating conditions. The proposed process is able to meet the same production of polysilicon as current traditional polysilicon facilities do, at a lower production cost since the benefits obtained from selling the high added value byproducts obtained increase the profit of the facility. The complete process, and therefore the operating conditions of each unit of the process were optimized under the objective of the maximization profit of the process. The optimal operating conditions of the facility that guarantee a lower energetic consumption, meeting with the required production of polycrystalline silicon require the production of high valuable byproducts as TEOS 99.5, and  $\text{SiH}_4$ , which aid in the economic sustainability of the process. The results after operating expenses, and considering the sale of polycrystalline silicon and the byproducts of the process, have an operational cost of 16.09 M\$/y. The total costs of equipment for the process is 85.93M\$, obtaining a competitive production cost for polycrystalline silicon of 6.86 \$/kg, below the commercial price estimated at 10 \$/kg, with the optimal production of 1875 kg/h of polycrystalline silicon and the byproducts optimal production of 26.91 kg/h of TEOS 99.5 and 4.595 kg/h of  $\text{SiH}_4$ . With these premises in hand, we conclude by describing the avenues for future research based on testing, modifying, and extending our conceptualization of the supply chain for the multiproduct polycrystalline silicon facility, and the analysis and treatment of waste stream costs.

#### ■ ASSOCIATED CONTENT

##### SI Supporting Information

The Supporting Information is available free of charge at <https://pubs.acs.org/doi/10.1021/acs.iecr.0c01006>.

Surrogate model development and validation (PDF)

#### ■ AUTHOR INFORMATION

##### Corresponding Authors

**Juan Gabriel Segovia-Hernández** – *Universidad de Guanajuato, Campus Guanajuato, División de Ciencias Naturales y Exactas, Departamento de Ingeniería Química, Guanajuato, Guanajuato 20256, México*; Email: [gsegovia@ugtomx.onmicrosoft.com](mailto:gsegovia@ugtomx.onmicrosoft.com)

**Mariano Martín** – *Universidad de Salamanca, Departamento de Ingeniería Química, Salamanca 37008, Spain*; [orcid.org/0000-0001-8554-4813](https://orcid.org/0000-0001-8554-4813); Email: [mariano.m3@usal.es](mailto:mariano.m3@usal.es)

#### Authors

**César Ramírez-Márquez** – *Universidad de Guanajuato, Campus Guanajuato, División de Ciencias Naturales y Exactas, Departamento de Ingeniería Química, Guanajuato, Guanajuato 20256, México*

**Edgar Martín-Hernández** – *Universidad de Salamanca, Departamento de Ingeniería Química, Salamanca 37008, Spain*

Complete contact information is available at: <https://pubs.acs.org/10.1021/acs.iecr.0c01006>

#### Notes

The authors declare no competing financial interest.

#### ■ ACKNOWLEDGMENTS

The authors acknowledge CONACyT (Mexico), Universidad de Guanajuato, and PSEM3 at Universidad de Salamanca.

#### ■ NOMENCLATURE

- $w$  = Total number of elements in the system
- $p$  = Price of each byproduct  $SP$  [\$/y]
- $dMO$  = Cost of manpower [\$/y]
- $c$  = Cost of each utility  $E$  [\$/y]
- $b$  = The unit cost of each raw material  $RM$  [\$/y]
- $a$  = Factor that considers annual expenses such as maintenance
- $W$  = Work exchanged by the system [kW]
- $Q$  = Heat exchanged by the system [kW]
- $z$  = Polytopic coefficient
- $x$  = Mole fraction
- $X$  = Amount of the specie [mass fraction]
- $wt$  = Weight percent
- TAC = Total Annual Cost
- $T$  = Temperature [K]
- RR = Reflux Ratio
- ROI = Return on investment
- Rel =  $\text{H}_2/\text{SiCl}_4$  molar feed ratio
- RD = Reactive Distillation
- $R$  = Molar gas constant [J/mol K]
- PV = Photovoltaic
- $P$  = Pressure [kPa]
- NLP = Nonlinear program
- kW = Kilowatt
- K = Kelvin
- HCl = Hydrogen chloride
- $\text{H}_2$  = Hydrogen
- GAMS = General Algebraic Modeling System
- FR = Feed Ratio
- FBR = Fluidized Bed Reactor
- $^\circ\text{C}$  = Celsius
- $\Delta H$  = Enthalpy variation [kJ/mol]
- $W_{(\text{Compressor})}$  = Electrical energy [kW]
- $T_{\text{outcompressor}}$  = Out temperature [K]
- $T_{\text{incompressor}}$  = Entry temperature [K]
- $T_{\text{RebCol}}$  = Bottom temperature [K]
- $T_{\text{ConCol}}$  = Top temperature [K]
- $S_{\text{polycrystalline silico}}$  = Profit from the sale of the polycrystalline silicon
- $Q_{\text{RebCol}}$  = Reboiler heat duty [kW]
- $Q_{\text{ConCol}}$  = Condenser heat duty [kW]
- $P_{\text{outcompressor}}$  = Out pressure [kPa]
- $P^\circ$  = Standard-state pressure (100 kPa);
- $P_{\text{incompressor}}$  = Entry pressure [kPa]

$I_F$  = Fixed annualized investment

$y_i$  = Molar fraction of species  $i$

## REFERENCES

- (1) Darling, S. B.; You, F.; Veselka, T.; Velosa, A. Assumptions and the leveled cost of energy for photovoltaics. *Energy Environ. Sci.* **2011**, *4* (9), 3133–3139.
- (2) EPIA Sustainability Working Group Fact Sheet; European Photovoltaic Industry Association., 2011. <http://www.epia.org/news/fact-sheets/>.
- (3) Yue, D.; You, F.; Darling, S. B. Domestic and overseas manufacturing scenarios of silicon-based photovoltaics: Life cycle energy and environmental comparative analysis. *Sol. Energy* **2014**, *105*, 669–678.
- (4) IEA Trends in Photovoltaic Applications: Survey Report of Selected IEA Countries between 1992 and 2011. Report IEA-PVPST1-21:2012; International Energy Agency, 2012. [http://www.iea-pvps.org/index.php?id=92&eID=dam\\_frontend\\_push&docID=1239](http://www.iea-pvps.org/index.php?id=92&eID=dam_frontend_push&docID=1239).
- (5) Ciftja, A. *Refining and recycling of silicon: a review*; Fakultet for naturvitenskap og teknologi, 2008.
- (6) Chamness, L.; Tracy, D. *Polysilicon Manufacturing Trends*. Renewable Energy World, 2011; Issue 4, Volume 2011. <https://www.renewableenergyworld.com/2011/08/01/polysilicon-manufacturing-trends/#gref>.
- (7) Mints, P. *Photovoltaic Manufacturer Capacity, Shipments, Price & Revenues 2017/2018*. SPV Market Work, 2018.
- (8) , . Wacker to build silica plant in Tenn. *Rubber & Plastics News* **2016**. <https://www.rubbernews.com/article/20161214/NEWS/161219980/wacker-to-build-silica-plant-intenn>.
- (9) Ramírez-Márquez, C.; Otero, M. V.; Vázquez-Castillo, J. A.; Martín, M.; Segovia-Hernández, J. G. Process design and intensification for the production of solar grade silicon. *J. Cleaner Prod.* **2018**, *170*, 1579–1593.
- (10) *Coal explained*; U.S. Energy Information Administration, 2019. <https://www.eia.gov/energyexplained/coal/prices-and-outlook.php>.
- (11) *Silicon Dioxide*; American Elements, 2020. <https://www.americanelements.com/silicon-dioxide-7631-86-9>.
- (12) Focus Technology Co., 2020. Made-in-China Connecting Buyers with Chinese Suppliers. [https://www.made-in-china.com/products-search/hot-china-products/sic14\\_price.html](https://www.made-in-china.com/products-search/hot-china-products/sic14_price.html) (accessed January 13, 2020).
- (13) *Product Listing Policy*; Alibaba, 2019. <https://www.alibaba.com/product-detail/Ethanol-99-9-50036986093.html>.
- (14) Price of Nitrogen. *The Physics Factbook*; 2019. <https://hypertextbook.com/facts/2007/KarenFan.shtml>.
- (15) *Hydrogen & Fuel Cells*; NREL, 2020. <https://www.nrel.gov/hydrogen/production-cost-analysis.html> (accessed January 12, 2020).
- (16) *Electricity Prices*; Global Petrol Prices, 2019. [https://www.globalpetrolprices.com/electricity\\_prices/](https://www.globalpetrolprices.com/electricity_prices/).
- (17) *Process Water Price*; Intratec Solutions, 2020. <https://www.intratec.us/chemical-markets/process-water-price>.
- (18) TLV, 2020. Compañía Especialista en vapor <https://www.tlv.com/global/LA/calculator/steam-unit-cost.html> (accessed January 13, 2020).
- (19) Wai, C. M.; Hutchison, S. G. Free energy minimization calculation of complex chemical equilibria: Reduction of silicon dioxide with carbon at high temperature. *J. Chem. Educ.* **1989**, *66* (7), 546.
- (20) Enríquez-Berciano, J. L.; Tremps-Guerra, E.; Fernández-Segovia, D.; de Elío de Bengy, S. *Monografías sobre Tecnología del Acero*; Parte III: Colada del acero. Universidad Politécnica de Madrid, 2009.
- (21) Ceccaroli, B.; Lohne, O. Solar grade silicon feedstock. *Handbook of photovoltaic science and engineering*; Wiley, 2003; pp 153–204.
- (22) Ding, W. J.; Yan, J. M.; Xiao, W. D. Hydrogenation of silicon tetrachloride in the presence of silicon: thermodynamic and experimental investigation. *Ind. Eng. Chem. Res.* **2014**, *53* (27), 10943–10953.
- (23) Payo, M. J. R. Purificación de triclorosilano por destilación en el proceso de obtención de silicio de grado solar. Ph.D. Dissertation, Universidad Complutense de Madrid, 2008.
- (24) Martín, M. *Industrial Chemical process. Analysis and Design*; Elsevier: Oxford, 2016.
- (25) Ramírez-Márquez, C.; Martín-Hernández, E.; Martín, M.; Segovia-Hernández, J. G. Optimal Design of a Multi-Product Polycrystalline Silicon Facility. *AICHE Annual Meeting, November 10–15, 2019*, Orlando, Florida.
- (26) Brage, F. J. P. *Contribución al modelado matemático de algunos problemas en la metalurgia del silicio*. Ph.D. Dissertation, Universidade de Santiago de Compostela, 2003.
- (27) Ramírez-Márquez, C.; Contreras-Zarazúa, G.; Martín, M.; Segovia-Hernández, J. G. Safety, Economic, and Environmental Optimization Applied to Three Processes for the Production of Solar-Grade Silicon. *ACS Sustainable Chem. Eng.* **2019**, *7* (5), 5355–5366.
- (28) Sánchez-Ramírez, E.; Ramírez-Márquez, C.; Quiroz-Ramírez, J. J.; Contreras-Zarazúa, G.; Segovia-Hernández, J. G.; Cervantes-Jauregui, J. A. Reactive Distillation Column Design for Tetraethoxysilane (TEOS) Production: Economic and Environmental Aspects. *Ind. Eng. Chem. Res.* **2018**, *57* (14), 5024–5034.
- (29) Ramírez-Márquez, C.; Sánchez-Ramírez, E.; Quiroz-Ramírez, J. J.; Gómez-Castro, F. L.; Ramírez-Corona, N.; Cervantes-Jauregui, J. A.; Segovia-Hernández, J. G. Dynamic behavior of a multi-tasking reactive distillation column for production of silane, dichlorosilane and monochlorosilane. *Chem. Eng. Process.* **2016**, *108*, 125–138.
- (30) Ramos, A.; Filtvedt, W. O.; Lindholm, D.; Ramachandran, P. A.; Rodríguez, A.; Del Cañizo, C. Deposition reactors for solar grade silicon: A comparative thermal analysis of a Siemens reactor and a fluidized bed reactor. *J. Cryst. Growth* **2015**, *431*, 1–9.
- (31) Del Coso, G.; Del Canizo, C.; Luque, A. Chemical vapor deposition model of polysilicon in a trichlorosilane and hydrogen system. *J. Electrochem. Soc.* **2008**, *155* (6), D485–D491.
- (32) Walas, S. M. *Chemical process equipment; selection and design*; Butterworth-Heinemann, 1988; No. 660.28 W3.
- (33) Turton, R.; Bailie, R. C.; Whiting, W. B.; Shaeiwitz, J. A.; Bhattacharyya, D. *Analysis, Synthesis and Design of Chemical Processes*; Pearson Education, 2012.
- (34) Alibaba, 2019. Product Listing Policy. [https://www.alibaba.com/product-detail/REACH-verified-producer-supply-HighQuality\\_60719460163.html?spm=a2700.7724857.normalList.2.2d6a243cK662pK&bypass=true](https://www.alibaba.com/product-detail/REACH-verified-producer-supply-HighQuality_60719460163.html?spm=a2700.7724857.normalList.2.2d6a243cK662pK&bypass=true) (accessed December 8, 2019).
- (35) Alibaba, 2019. Product Listing Policy. <https://www.alibaba.com/product-detail/Tetraethyl-orthosilicate-TEOS-CAS-78-10-1299681072.html?spm=a2700.7724857.normalList.2.12192296hSVZQb&s=p> (accessed December 8, 2019).
- (36) Alibaba, 2019. Product Listing Policy. <https://spanish.alibaba.com/product-detail/cas-78-10-4-super-low-price-tetraethylsilane-tetraethyl-orthosilicate-60813279070.html?spm=a2700.8699010.normalList.29.1eac341fplwUSq> (accessed December 8, 2019).
- (37) Focus Technology Co., 2020. Made-in-China Connecting Buyers with Chinese Suppliers. <https://dswgascylinder.en.made-in-china.com/product/pCAmYnLFluHl/China-99-9999-Sih4-Silane.html> (accessed December 8, 2019).
- (38) *Dichlorosilane*; American Elements, 2020. <https://www.americanelements.com/dichlorosilane-4109-96-0>.
- (39) *Chlorosilane*; Zibo Hangyu Import&Export Co., Ltd, 2020. <https://hangyuchemical.lookchem.com/products/CasNo-13465-78-6-Chlorosilane-23107353.html>.
- (40) Sartori, D.; Catalano, G.; Genco, M.; Pancotti, C.; Sirtori, E.; Vignetti, S.; Del Bo, C. Guide to cost-benefit analysis of investment projects. *Economic appraisal tool for Cohesion Policy*, 2020; European Commission, 2014.
- (41) Guide to cost-benefit analysis of investment projects. *Economic appraisal tool for Cohesion Policy*; European Commission, 2008.

(42) PVinsights Grid the world. United States of America Publishing. PVinsights, 2019. <http://pvinsights.com/> (accessed January 13, 2020).

(43) Marked Research Consulting. AMPLE, 2020. [amplemarketreports.com/report/global-tetraethyl-orthosilicate-market-497751.html](http://amplemarketreports.com/report/global-tetraethyl-orthosilicate-market-497751.html) (accessed January 13, 2020).

(44) Trichlorosilane (TCS) Market - Global Industry Analysis, Size, Share, Growth, Trends and Forecast 2016 - 2024. Transparency Market Research, 2020. <https://www.transparencymarketresearch.com/trichlorosilane-market.html> (accessed January 13, 2020).